Meteoritics & Planetary Science 40, Nr 6, 795–804 (2005)
Abstract available online at http://meteoritics.org

The Villalbeto de la Peña meteorite fall: I. Fireball energy, meteorite recovery, strewn field, and petrography

Jordi LLORCA[1, 2*], Josep M. TRIGO-RODRÍGUEZ[3], José L. ORTIZ[4], José A. DOCOBO[5], Javier GARCÍA-GUINEA[6], Alberto J. CASTRO-TIRADO[4], Alan E. RUBIN[3], Otto EUGSTER[7], Wayne EDWARDS[8], Matthias LAUBENSTEIN[9], and Ignasi CASANOVA[10]

[1]Departament de Química Inorgànica, Universitat de Barcelona, Barcelona, Spain
[2]Institut d'Estudis Espacials de Catalunya, Barcelona, Spain
[3]Institute of Geophysics and Planetary Physics, University of California at Los Angeles, USA
[4]Instituto de Astrofísica de Andalucía, CSIC, Granada, Spain
[5]Observatorio Astronómico Ramón Maria Aller, Universidade Santiago de Compostela, Santiago de Compostela, Spain
[6]Museo Nacional de Ciencias Naturales, Madrid, Spain
[7]Physikalisches Institut, University of Bern, Berne, Switzerland
[8]Department of Earth Sciences, University of Western Ontario, London, Ontario, Canada
[9]Laboratori Nazionali del Gran Sasso, Istituto Nazionale di Fisica Nucleare, Rome, Italy
[10]Group of Mechanics and Nanotechnology of Engineering Materials, Universitat Politècnica de Catalunya, Barcelona, Spain
*Corresponding author. E-mail: jordi.llorca@qi.ub.es

This article is dedicated to the memory of Professor Alfredo San Miguel (1917–2004).

(Received 10 February 2005; revision accepted 24 March 2005)

Abstract–An impressive daylight fireball was observed from Spain, Portugal, and the south of France at 16h46m45s UTC on January 4, 2004. The meteoroid penetrated into the atmosphere, generating shock waves that reached the ground and produced audible booms. The associated airwave was recorded at a seismic station located 90 km north of the fireball trajectory in Spain, and at an infrasound station in France located 750 km north-east of the fireball. The absolute magnitude of the bolide has been determined to be −18 ± 1 from a casual video record. The energy released in the atmosphere determined from photometric, seismic, and infrasound data was about 0.02 kilotons (kt). A massive fragmentation occurred at a height of 28 ± 0.2 km, resulting in a meteorite strewn field of 20 × 6 km. The first meteorite specimen was found on January 11, 2004, near the village of Villalbeto de la Peña, in northern Palencia (Spain). To date, about 4.6 kg of meteorite mass have been recovered during several recovery campaigns. The meteorite is a moderately shocked (S4) L6 ordinary chondrite with a cosmic-ray-exposure age of 48 ± 5 Ma. Radioisotope analysis shows that the original body had a mass of 760 ± 150 kg, which is in agreement with the estimated mass obtained from photometric and seismic measurements.

INTRODUCTION

Detection of daylight superbolides (fireballs with brightness greater than −17 visual magnitude) from the ground is an unusual phenomenon that can provide important information about the population of interplanetary bodies intercepting the Earth's orbit, the size of these bodies, and the impact energy released when they collide with the atmosphere. "Meteorite-dropping" fireballs have the added bonus of allowing the composition of the meteoroid to be determined. In this paper we study the L6 chondrite Villalbeto de la Peña that fell in northern Spain on January 04, 2004 (Russell et al. 2004). We first describe the superbolide and estimate the fireball energy released in the atmosphere from photometric, seismic, and infrasound data. Then we describe the meteorite recovery, strewn field geometry, meteorite petrology, chemical composition, and noble gas contents. Finally, we estimate the size of the meteoroid from the energy released and from cosmogenic radionuclide analysis. The atmospheric trajectory and heliocentric orbit of the meteoroid are currently being reconstructed on the basis of detailed astrometric stellar calibrations of video and photographic records. These results will be discussed in detail in a separate paper (Trigo-Rodríguez et al. 2005).

FIREBALL DESCRIPTION AND ENERGY RELEASE

The Villalbeto de la Peña fireball was observed at 16h46m45s ± 2s UTC on Sunday January 04, 2004. It was first seen over northern Portugal and traveled north-eastward, with a slope relative to the surface of ~30°, over several Spanish provinces: Zamora, León, and Palencia, resulting in a visible path about 150 km long. Because it appeared in daylight, the fireball was seen by thousands of people. Eyewitnesses' reports arrived even from sites located more than 600 km away (Fig. 1). The fireball was videotaped and photographed as it travelled over the León and Palencia provinces. The videotape recorded various explosions along the meteoroid's trajectory, with the main fragmentation occurring at an altitude of 28 ± 0.2 km. Thundering detonations were heard over a wide region, and several localities in León and Palencia provinces felt a strong pressure wave that made buildings shake and windows rattle. A long, smoky trail remained visible in the sky for nearly 35 minutes.

The video record from the city of León shows that the fireball was visible in daylight (Fig. 2). The mini digital video (MiniDV) tape was played back and the video was captured as an AVI file. From the AVI file, single frames were extracted for analysis. A total of 50 frames were used. Because the digital camera was of the scan mode rather than of full frame type, each frame consisted of two interlaced half-frames separated by 1/50 s. These frames were deinterlaced using linear interpolation, which resulted in a total of 100 images available for analysis. Each color frame was split into the three different channels: red, green, and blue (R, G, B). Because the sky was still bright at the time of the recording, all the blue images had a completely saturated background, which made the bolide hardly distinguishable. The G channel images were somewhat better, but the sky background was still very bright and therefore only the R channel images were selected for analysis. Although the sky background was not saturated in the R channel images, the center of the bolide was indeed strongly saturated in nearly all of the frames. Therefore, the photometric analysis was not straightforward. To carry out such analysis, point spread functions were fitted to the non-saturated areas of the bolide. Radially asymmetric Moffat point spread functions were applied; these are widely used to fit the intensity of stellar images in astronomical observations (Moffat 1969). The underlying assumption that the bolide is a point-like source was substantiated by the fact that the video resolution was not very high and, therefore, any plausible extended size of the bolide was still below the spatial resolution of the camera. Fortunately, the presence of the Moon in all the images allowed a convenient calibration relative to the Moon, whose R magnitude is known (on that date this was assumed to be 11.6 ± 0.1). A 6000 K blackbody emission was assumed to compute the flux emitted in the visible range (Brown et al. 2002a). The Villalbetode la Peña fireball had an absolute magnitude of −18 ± 1.

Fig. 1. A map of the Iberian Peninsula showing the projection of the Villalbeto de la Peña atmospheric trajectory on the Earth's surface and the video, photographic, and seismic locations from which the fireball was registered. An arrow indicates the direction to the infrasound station of Flers (France). Some visual eyewitnesses are also included.

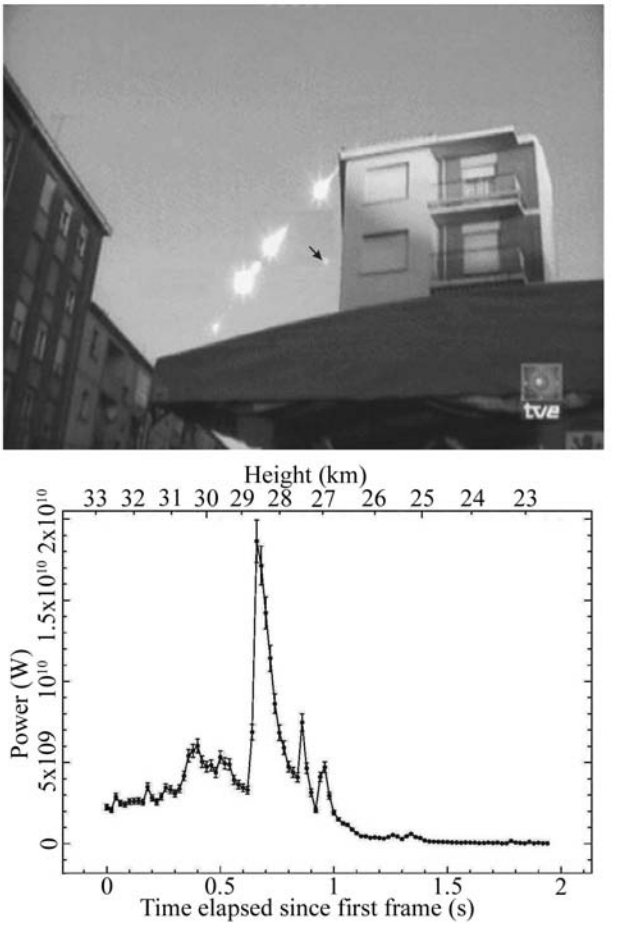

Fig. 2. Video sequence (superposed frames) and photometry of the last part of the fireball's trajectory (bolide height from Trigo-Rodríguez et al. 2005). An arrow marks the position of the Moon.

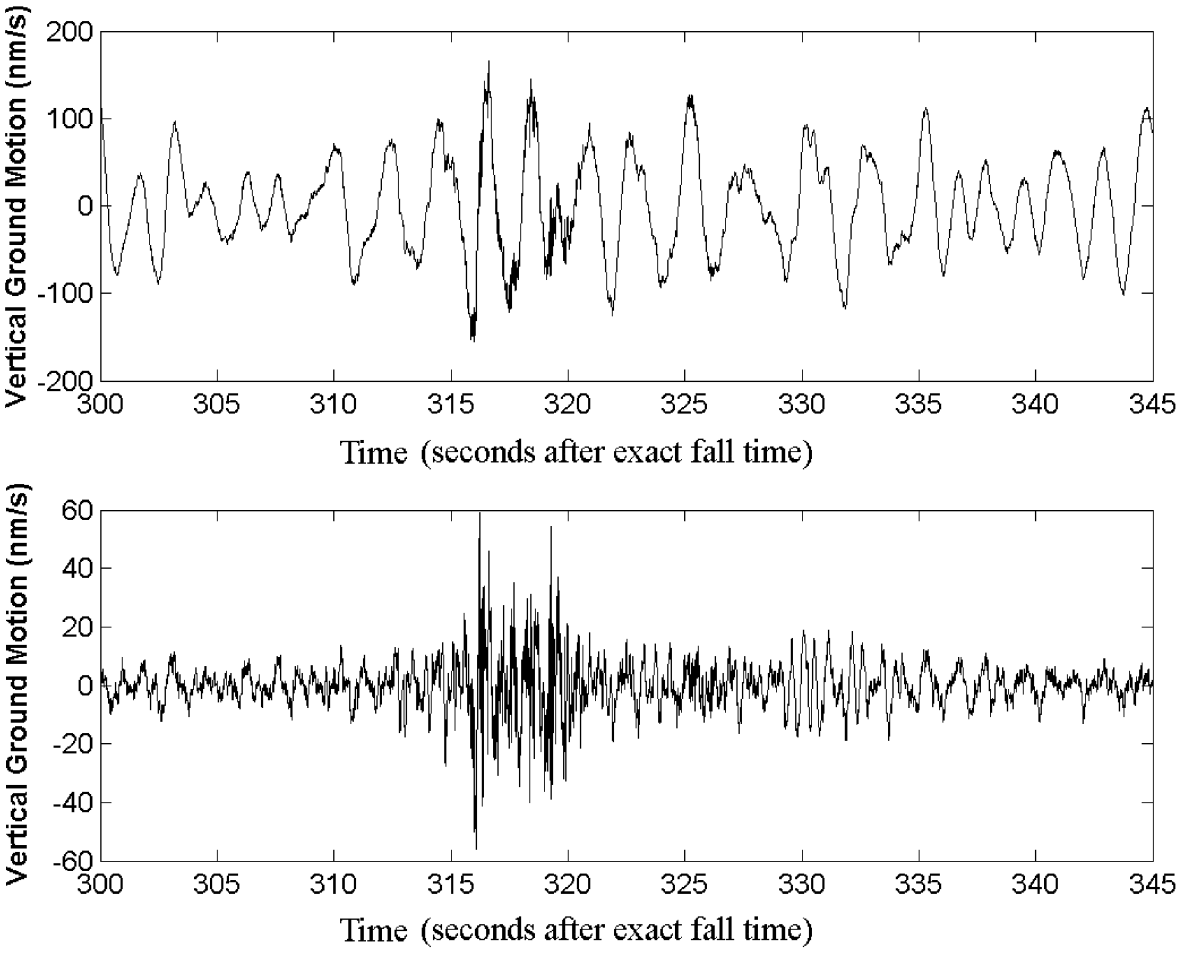

Fig. 3. Raw (above) and filtered (1.25–40 Hz; below) vertical ground motion recorded at the seismic station EARI of Arriondas (Spain) generated by the fireball.

In addition, the video record allowed accurate photometry of the fireball during the last part of its trajectory. The total energy emitted as light, obtained by integrating the data plotted in Fig. 2, was 5.21×10^9 J. The estimated luminous efficiency was derived from the equations of Brown et al. (2002a) yielding a value of 0.0562. The initial kinetic energy of the bolide was therefore 9.28×10^{10} J or 0.022 kt. Taking into account an estimated velocity at infinity to be 17 km s^{-1} (Trigo-Rodríguez et al. 2005), we determined an initial mass of about 640 kg.

SEISMIC AND INFRASOUND DETECTIONS

An airwave signal was received at the remote broadband seismic station EARI located in Arriondas, Spain (43.3°N and −5.21°E). At 16h51m58s UTC a sharp signal that lasted for about 30 s, with energy above 20 Hz, was recorded. The vertical component of this signal displays two distinct peaks, the first at 16h52m01.1s and the second at 16h52m04.0s UTC after application of a 1.25–40 Hz bandpass filter (Fig. 3). Both peaks show significant negative ground-motion velocity prior to their maxima, which is likely associated with an arriving positive overpressure of an airwave. Peak vertical ground motions for the two arrivals reached 59.0 and 54.6 nm s^{-1}, respectively. The source identification of the seismic signal was performed by geometric ray tracing using SUPRACENTER (Edwards et al. 2004) and an atmospheric model buildup by the Spanish National Institute of Meteorology for the region at 18h UTC. Discrete points along the fireball's trajectory (including the locations of the main fragmentation and final visual observation) were chosen as potential source positions for the acoustic wave. Theoretical acoustic arrival times were compared with the measured seismic arrivals and the region associated with the trajectory at an altitude of 28–29 km was delimited. This part of the trajectory was situated at a range of ~90 km from EARI near the periphery of the direct arrival shadow zone. Ray orientations (358° azimuth, 32.4° elevation) indicate that a point source associated with the main bolide fragmentation, and not a ballistic airwave, is the most likely source for the

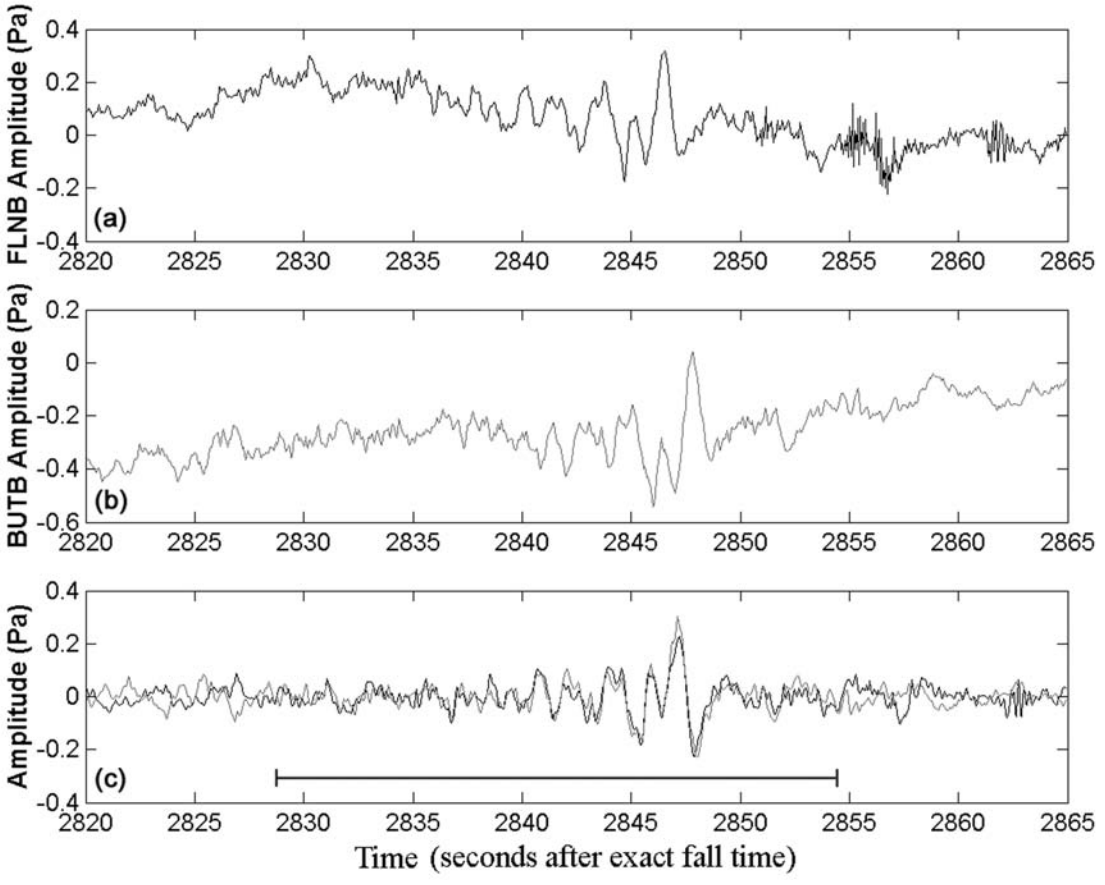

Fig. 4. Infrasound signal recorded at Flers microbarometer array (France): a) Raw channel FLNB; b) Raw channel BUTB; c) Phase-aligned and bandpass-filtered channels (0.2–5 Hz). The approximate duration of the signal is shown as a black bar.

acoustic wave. An estimate for the initial energy of the bolide from seismic data was also performed using the equation of Brown et al. (2002b). Using the same values for seismic to acoustic efficiency, the same attenuation factor used during analysis of the Tagish Lake seismic recordings (Brown et al. 2002b), and the average vertical ground motion during the first peak observed at EARI (40.6 nm s^{-1}) at a range of 90 km, we determined a value of 0.020 kt for the Villalbeto de la Peña bolide. This result is in excellent agreement with the photmetric data.

With the detection of a seismically-coupled airwave with an energy content below 20 Hz, we anticipated that some of the sub-acoustic sound could have been propagated to even greater ranges. Bolides have been shown to be a natural source of infrasound; detections by arrays of microbarometers have been well documented (e.g., Le Pichon et al. 2002; Brown et al. 2002c; Evers et al. 2003). In the case of the Villalbeto de la Peña bolide, a search for potential detections was made at several of the nearest infrasound arrays in Europe. Of these, Flers array in Normandy, France (48.76°N, 0.48°W), was the only one to show signs of a potential detection at an observational range of ~750 km. The signal, identified by a brief increase in cross-correlation, arrived at approximately 17h33m53s UTC and lasted for ~26 s with a maximum peak to peak amplitude of 0.47 ± 0.07 Pa and a period at maximum amplitude of 2.3 ± 0.3 s with an integrated energy signal to noise ratio of 11.8 ± 0.5 (Fig. 4). The signal would have been a strong downwind (48.3 m s^{-1}) observation according to the average modelled HWM stratospheric winds (Hedin et al. 1996) along the Villalbeto de la Peña to Flers propagation path. This may explain the significant frequency content of up to ~3 Hz as a result of stratospheric wave guide focusing due to high winds. Unfortunately, at the time of the anticipated arrival of the airwave, only two of the Flers array elements were operational; this made it impossible to determine the direction from which the signal originated as is commonly done using array element cross-correlation (Evers et al. 2001). However, if a trace velocity (apparent signal velocity across the array) of 0.350 km s^{-1} is assumed, typical of a stratospherically ducted wave, and the arrival azimuth is varied until the two channel wave forms become aligned in phase (Fig. 4), a back azimuth of 201 ± 10° is found. This is consistent with the 208° back azimuth anticipated for a signal from Villalbeto de la Peña arriving at Flers. With this excellent back azimuth agreement coupled with signal properties (which are

Table 1. Mean compositions (wt%) of silicate phases and chromite.

	Olivine	Low-Ca pyroxene	Plagioclase	Chromite
Nr. of grains	10	5	5	6
SiO_2	37.9 ± 0.3	54.9 ± 0.3	65.6 ± 0.7	0.04 ± 0.03
TiO_2	<0.04	0.16 ± 0.02	<0.04	2.9 ± 0.2
Al_2O_3	0.04	0.15 ± 0.03	23.4 ± 0.1	5.9 ± 0.1
Cr_2O_3	<0.04	0.10 ± 0.05	<0.04	57.0 ± 0.3
FeO	22.3 ± 0.3	13.7 ± 0.2	0.37 ± 0.15	30.8 ± 0.4
MnO	0.46 ± 0.03	0.47 ± 0.05	<0.04	0.82 ± 0.06
MgO	39.3 ± 0.3	29.5 ± 0.1	<0.04	2.6 ± 0.2
CaO	0.04	0.84 ± 0.09	2.3 ± 0.1	0.04 ± 0.01
Na_2O	0.04	<0.04	7.4 ± 0.5	0.05 ± 0.02
K_2O	0.04	<0.04	1.2 ± 0.3	0.04 ± 0.01
Total	100.1	99.8	100.3	100.2
End-member	Fa 24.2 ± 0.2	Fs 20.4 ± 0.1	Ab 69.2 ± 2.1	
		Wo 1.6 ± 0.2	Or 7.3 ± 1.7	

consistent with a 0.021 kt bolide), we are confident that the signal observed at Flers likely had its source at the Villalbeto de la Peña bolide.

If this interpretation is correct, then the observed signal properties can be used with various empirical energy relations to estimate the bolide energy. One of these methods is the AFTAC period at maximum amplitude relation for yields <100 kt (ReVelle 1997) derived from ground based nuclear data. Using this relation, we find the energy to be 0.085 ± 0.037 kt for the Villalbeto de la Peña bolide. This estimate, a factor of four larger than the value obtained from photometric and seismic data, may be viewed as an extreme upper limit to the source energy since many effects (such as the presence of strong winds) may change the observed period (ReVelle 1976). Other methods, derived from previously observed bolide infrasound and optical satellite data, are the recent signal property relations of Edwards et al. (2005). Using these relations and the wind estimates discussed above, the bolide's source energy is estimated to be about 0.018 kt. Taking into account that there remains a fair amount of uncertainty in the regression parameters of the Edwards et al. (2005) relations, we find that the fireball energy obtained from infrasound data is in good agreement with both the luminous efficiency and seismic amplitude estimates.

METEORITE RECOVERY, PETROLOGY, CHEMICAL ANALYSIS, AND NOBLE GASES

By the middle of January 2004, a preliminary estimate of the fireball atmospheric trajectory from all available observations (compiled by the Spanish Photographic Meteor Network) was successfully used to constrain the meteorite's impact area for the purpose of meteorite recovery tasks. The first specimen, covered with a shiny, black fusion crust, was found on January 11, 2004, near Villalbeto de la Peña in northern Palencia (Spain) by a local resident. In the following weeks our team carried out an intensive recovery campaign to collect all possible specimens and to determine their exact positions. Meteorite hunters also found specimens and removed them from the field. Due to the small slope of the atmospheric trajectory and numerous fragmentation events, the recovered specimens (4.6 kg total) were dispersed over a large impact area. The strewn field covered a sparsely-populated area of about 20 × 6 km. The location and weight of each recovered specimen (32 pieces have been recovered to date) are summarized in Fig. 5. All of them have black fusion crusts; some possess double fusion crusts produced by different phases of ablation (Fig. 6).

The bulk density of the meteorite is 3.42 g cm^{-3}, which is within the 3.40 ± 0.15 g cm^{-3} range for L6 chondrites (Wilkinson et al. 2000). Numerous shock veins are present. The meteorite contains ~2–3 vol% metallic Fe-Ni, occurring as kamacite (6.9 ± 0.5 wt% Ni, 1.0 ± 0.1 wt% Co), taenite (37.6 ± 1.9 wt% Ni, 0.3 ± 0.05 wt% Co), and plessite. The composition of troilite is very homogeneous (63.3 ± 0.2 wt% Fe, 36.7 ± 0.2 wt% S). Electron microprobe analyses (Table 1) of the olivine (Fa 24.2 ± 0.2 mol%) and low-Ca pyroxene (Fs 20.3 ± 0.2, Wo 1.6 ± 0.2 mol%) are in the range of L-group chondrites (Fa 23.0–25.8, Fs 18.7–22.6; Rubin 1990; Gomes et al. 1980). Although the mean chromite composition differs somewhat from mean L-chondrite chromite, each of the oxide components are in the ranges for L4–6 chondrites (Bunch et al. 1967). The homogeneity of the mafic silicate compositions, the occurrence of 50-μm-size plagioclase grains, (Fig. 7) and recrystallized texture (Fig. 8) indicate petrologic type 6. The occurrence of weak mosaicism and sets of planar fractures in the olivine grains indicates that the rock is of shock stage S4 (Stöffler et al. 1991). Plagioclase in Villalbeto de la Peña (Ab 69.2 Or 7.3) differs from the mean composition in equilibrated L chondrites (Ab 84.2 Or 5.6; van Schmus et al. 1968) in being depleted in Na_2O and enriched in K_2O. This compositional difference could result from preferred shock volatilization of Na plagioclase (Rubin 1985).

The concentrations and isotopic compositions of He, Ne, and Ar were determined in two bulk samples (Table 2). The

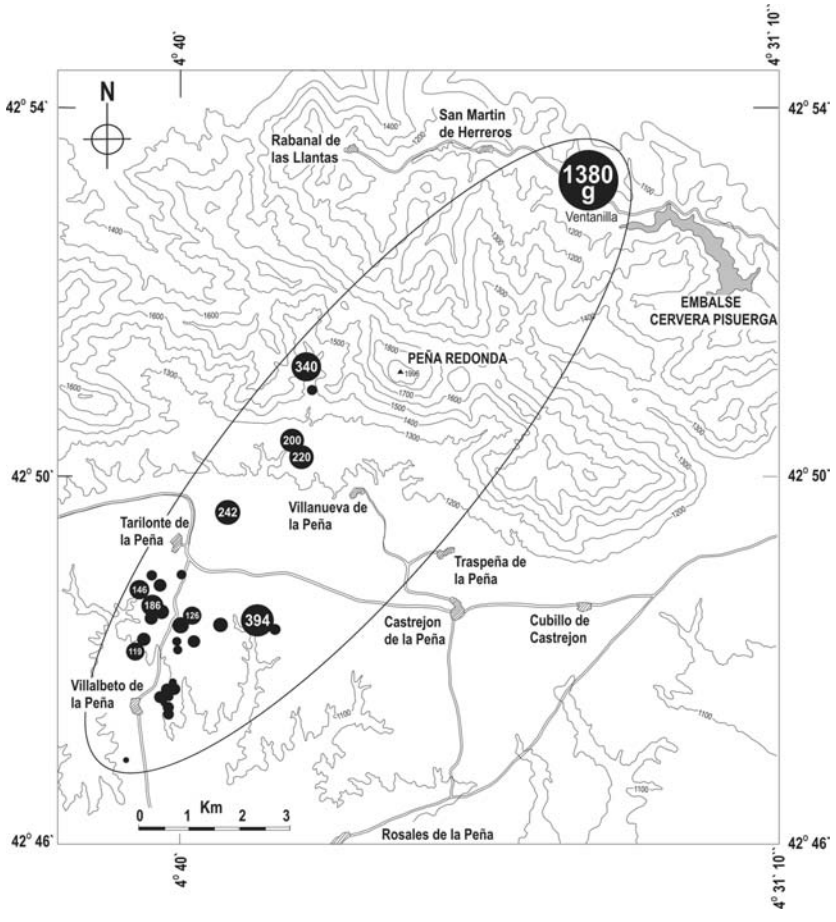

Fig. 5. Strewn field of the Villalbeto de la Peña meteorite fall showing the position of the recovered specimens. The area of the circles is proportional to the specimen weight: Numbers indicate weights for stones >100 g.

Fig. 6. Images of several Villalbeto de la Peña meteorite specimens from the Museo Nacional de Ciencias Naturales of Madrid (host institution). The image on the bottom right shows a specimen with a double fusion crust, supporting the observation of multiple fragmentation events during the atmospheric flight.

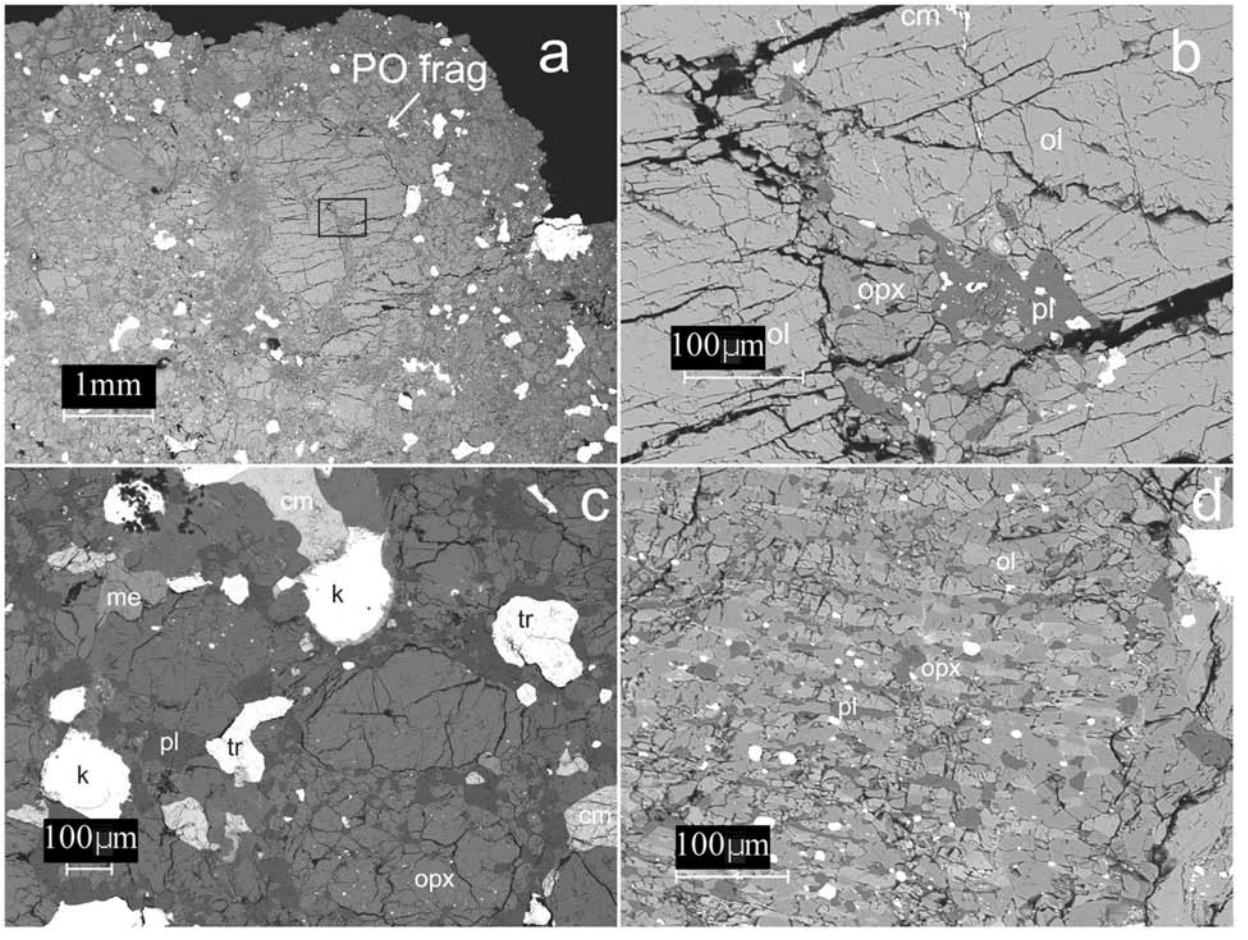

Fig. 7. Backscattered electron images of the Villalbeto de la Peña meteorite: a) Portion showing a recrystallized porphyritic olivine chondrule fragment. White grains are metallic Fe-Ni, troilite and chromite. b) Area outlined in Fig. 7a showing a plagioclase-rich melt (pl), numerous impact-induced fractures (black) and coarse grains of olivine (ol) and orthopyroxene (opx). c) Typical recrystallized region showing: kamacite (k), troilite (tr), chromite (cm) and merrillite (me). d) Recrystallized barred olivine chondrule with discontinuous olivine bars, intercalated orthopyroxene, and blebs of metallic Fe-Ni (white).

Table 2. Results of He, Ne, and Ar measurements (in 10^{-8}cm^{3}STP/g).

Sample weight (mg)	^{4}He	^{20}Ne	^{40}Ar	^{4}He/^{3}He	^{20}Ne/^{22}Ne	^{22}Ne/^{21}Ne	^{36}Ar/^{38}Ar	^{40}Ar/^{36}Ar
20.4	530 ± 20	17.6 ± 0.5	304 ± 10	6.44 ± 0.08	0.853 ± 0.008	1.059 ± 0.005	1.145 ± 0.020	97.2 ± 2.0
30.2	570 ± 20	18.9 ± 0.6	287 ± 10	6.48 ± 0.08	0.851 ± 0.008	1.059 ± 0.005	1.199 ± 0.020	88.7 ± 2.0
Average	550 ± 20	18.2 ± 0.7	295 ± 10	6.46 ± 0.08	0.852 ± 0.008	1.059 ± 0.005	1.172 ± 0.020	93.0 ± 5.0

techniques and methods are described in Eugster et al. (1993). The concentration of cosmogenic, trapped, and radiogenic noble gases are given in Table 3. Based on the cosmogenic noble gas data and on the method proposed by Eugster (1988), an average cosmic-ray exposure (CRE) age of 48 ± 5 Ma was obtained (Table 4). This is the duration that the original meteoroid spent in interplanetary space as a meter-sized object. There are ~10 other L chondrites with a CRE age of about 48 Ma, but a major peak is around 40 Ma and a broad one around 28 Ma. According to Marti et al. (1992), a major collisional event ~40 Ma ago produced mainly chondrites of petrographic type L6. As expected, CRE ages obtained independently from ^{3}He, ^{21}Ne, and ^{38}Ar (T_3, T_{21}, and T_{38} respectively; Table 4) show the characteristics of a fresh fall (T_3 and T_{38} are not lower than T_{21}). The ^{40}Ar content is low and corresponds to a K-Ar gas retention age of about 700 Ma. The low ^{4}He and ^{40}Ar contents indicate gas loss due to heating on the asteroid before ejection. During transfer from the asteroid to Earth, no heating and gas loss occurred, as shown by the normal ^{3}He CRE age. The cosmogenic ^{22}Ne/^{21}Ne ratio of 1.05 is the same as that of the L6 chondrite Walters, which had a pre-atmospheric mass of >300 kg (Eugster et al. 1993). The trapped ^{36}Ar content is typical for type 6 chondrites.

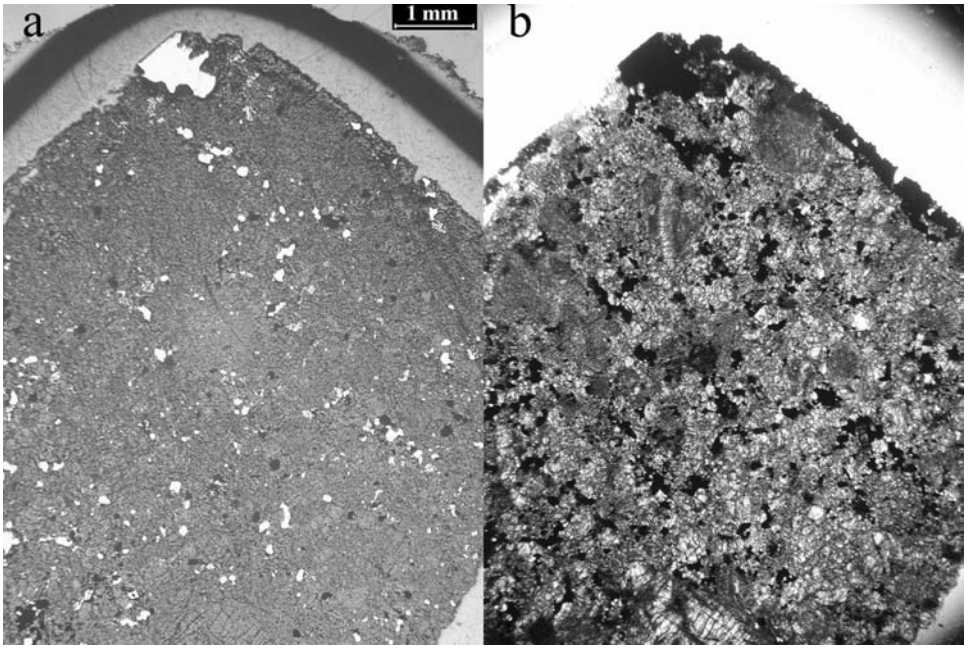

Fig. 8. Thin section photographs of Villalbeto de la Peña. (a) Reflected light image showing metal grains (white), troilite (light gray), and silicate (medium gray). (b) Transmitted light image of the same view showing the recrystallized texture.

Table 3. Cosmogenic, trapped, and radiogenic components of He, Ne, and Ar[a].

Cosmogenic				Trapped		Radiogenic	
^{3}He	^{21}Ne	^{38}Ar	^{22}Ne/^{21}Ne	^{20}Ne	^{36}Ar	^{4}He	^{40}Ar
85.1 ± 4.0	20.2 ± 0.3	2.41 ± 0.20	1.05 ± 0.006	1.2 ± 0.7	1.6 ± 0.2	<40	295 ± 10

[a] Assumptions: $^{4}He_{tr}$=0, $(^{4}He/^{3}He)_{c}$ = 6.2 (Welten et al. 2003); $(^{20}Ne/^{22}Ne)_{tr}$ = 8.4; $(^{22}Ne/^{21}Ne)_{tr}$ = 0.035 (Tang et al. 1988); $(^{20}Ne/^{22}Ne)_{c}$ = 0.80; $(^{36}Ar/^{38}Ar)_{c}$ = 0.65, $(^{36}Ar/^{38}Ar)_{tr}$ = 5.32, $(^{40}Ar/^{38}Ar)_{c}$ = 0.2. Concentrations in 10^{-8}cm^{3} STP/g.

Table 4. Production rates (in 10^{-8}cm^{3} STP/g) and CRE ages (in Ma).

P_3	P_{21}	P_{38}	T_3	T_{21}	T_{38}	T_{av}
1.638 ± 0.160	0.455 ± 0.045	0.0504 ± 0.0050	52.0 ± 8.0	44.4 ± 6.5	47.8 ± 7.0	48.1 ± 5.0

COSMOGENIC RADIONUCLIDES

Two bulk samples of the Villalbeto de la Peña meteorite were analyzed shortly after the fall by means of non-destructive gamma spectrometry using a high-purity Ge detector. The techniques and methods are described in Laubenstein et al. (2004). The measured activity concentrations for cosmogenic radionuclides are summarized in Table 5. The presence of the short-lived radionuclide ^{48}V ($t_{½}$~16 days) clearly indicates freshly fallen samples. Only ^{26}Al lives long enough to ensure that the variation of the galactic cosmic-ray fluxes are averaged out. Therefore, the other shorter lived nuclides were normalized in their concentrations to the ones of the target elements from which they were produced. We assumed an average L-chondrite composition (Jarosewich 1990). Comparing these normalized concentrations with model calculations for cosmogenic production rates in stony meteorites (Leya et al. 2000), we deduced that for ^{26}Al, ^{57}Co and ^{54}Mn, the maximal possible productions rates were reached in both samples. This leads to the conclusion that they were in the central positions of a meteoroid with a radius between 30 and 50 cm. Also, the measured normalized concentration of ^{44}Ti gives a radius of about 40 cm (with a large uncertainty) (Michel et al. 1998). According to Eberhardt et al. (1963) and Alexeev et al. (2001), ^{60}Co is the most sensitive depth indicator; in our case it fixes the pre-atmospheric radius between 35 and 40 cm (610 kg to 910 kg), in good agreement with photometric and seismic data.

The concentrations of the natural radionuclide ^{232}Th of $(61 \pm 7 \times 10^{-9}$ g/g (small sample) and $(42 \pm 2) \times 10^{-9}$ g/g (large sample) are consistent with the average content of chondrites (42×10^{-9} g/g) (Alexeev et al. 2001). The measured concentrations of K_{nat} of $(1020 \pm 70) \times 10^{-6}$ g/g and $(1000 \pm 70) \times 10^{-6}$ g/g for the small and large sample, respectively, are also in very good agreement with the assumed average concentration (913×10^{-6} g/g). All of the analyzed radionuclides show concentrations close to the

Table 5. Activity concentrations of cosmogenic radionuclides.

Nuclide	Activity concentrations (dpm/kg)[a] 38.1 g sample	119.1 g sample
^{7}Be	123 ± 15	102 ± 12
^{22}Na	265 ± 8	255 ± 6
^{26}Al	76 ± 32	80 ± 2
^{44}Ti	1.6 ± 0.7	1.3 ± 0.5
^{46}Sc	8.8 ± 1.0	8.7 ± 0.8
^{48}V	16 ± 3	16 ± 4
^{51}Cr	110 ± 19	72 ± 20
^{54}Mn	126 ± 3	130 ± 2
^{56}Co	4.8 ± 0.9	5.5 ± 0.6
^{57}Co	17.4 ± 1.0	15.8 ± 0.9
^{58}Co	17.2 ± 1.8	13.2 ± 1.3
^{60}Co	79 ± 3	71 ± 2

[a]The reported errors are expanded uncertainties with k = 1.

average except for ^{22}Na, which shows a peculiarly high value—almost three times the maximum expected value for ordinary chondrites (Bhandari et al. 1993). This is very difficult to explain because ^{22}Na and ^{26}Al are normally assumed to vary similarly with shielding, and in this case the ^{26}Al value behaves regularly but the ^{22}Na is far off of the average. Possible explanations could be either a break-up episode shortly before entering the atmosphere that could influence the radionuclide concentration (Evans et al. 1982), or an uncertainty in the cross sections for the production of ^{22}Na from its mother products Si, Al, and Mg (Sisterson et al. 2004).

CONCLUSIONS

The Villalbeto de la Peña meteorite is an L6 (S4) chondrite with a CRE age of 48 ± 5 Ma and a K-Ar gas retention age of about 700 Ma. Based on the analysis of luminosity, seismic, and infrasound data, the initial pre-atmospheric mass of Villalbeto de la Peña was ~760 ± 150 kg. This value corresponds to a body of about 0.8 m in diameter (assuming a bulk density of 3.4 g cm^{-3}), and it is completely consistent with the deduced meteoroid size from ^{60}Co activity. The main fragmentation of the meteoroid occurred at a height of 28 ± 0.2 km and released an amount of energy equivalent to ~0.02 kt. Meteorite fragments were scattered in a strewn field of about 95 km^2.

Acknowledgments–We thank Bartolomé Orfila and Juan Guerra of the Instituto Nacional de Meteorología for providing atmospheric profiles, Emilio Carreño of the Red Sismológica Española for providing seismic data, and Alexis Le Pichon for providing data and valuable discussions about the Flers infrasound station. Yuri Vinogradov of the Russian Academy of Sciences provided infrasonic data from the Apatity array. We also thank José V. Casado, Saúl Blanco, Ricardo Chao, Stanislaus Erbrink, Martín Fernández, Virgilio Correcher, José L. Allende, Abel Tarilonte, and additional volunteers of the Asociación Leonesa de Astronomía and the Agrupación Astronómica Palentina for their participation in the recovery tasks. We are indebted to Luis A. Fernández, Carmen Blanco, and Televisión Española for providing us with the original video. Pablo Santos and José A. Quesada are acknowledged for their assistance in the early part of this investigation. We also acknowledge the data provided by Rainer Bartoschewitz, Jürgen Neu, Pierre M. Pele, Steffen Jacobsen, Thomas Grau, and other anonymous finders about the weight and location of specimens collected by them. Financial support from MEC AYA2004-20101-E is acknowledged. J. Llorca is also grateful to MCYT and DURSI (Generalitat de Catalunya). J. M. Trigo-Rodrígez thanks the Spanish State Secretary of Education and Universities for a postdoctoral grant. J. L. Ortiz is grateful to AYA-2002-00382.

Editorial Handling—Dr. Walter Huebner

REFERENCES

Alexeev V. A., Goron V. D., and Usnitova G. K. 2001. The Kunya-Urgench and some other fresh-fallen chondrites: Cosmogenic radionuclides (abstract #1024). 32nd Lunar and Planetary Science Conference. CD-ROM.

Bandhari N., Mathew K. J., Rao M. N., Herpers U., Bremer K., Vogt S., Wolfli W., Hofmann H. J., Michel R., Bodemann R., and Lange H.-J. 1993. Depth and size dependence of cosmogenic nuclide production rates in stony meteoroids. *Geochimica et Cosmochimica Acta* 57:2361–2375.

Brown P. G., Spalding R. E., ReVelle D. O., Tagliaferri E., and Worden S. P. 2002a. The flux of small near-Earth objects colliding with the Earth. *Nature* 420:294–296.

Brown P. G., ReVelle D. O., Tagliaferri E., and Hildebrand A. R. 2002b. An entry model for the Tagish Lake fireball using seismic, satellite, and infrasound records. *Meteoritics & Planetary Science* 37:661–675.

Brown P. G., Whitaker R. W., ReVelle D. O., and Tagliaferri E. 2002c. Multi-station infrasonic observations of two large bolides: Signal interpretation and implications for monitoring of atmospheric explosions. *Geophysical Research Letters* 29, doi:10.1029/2001GL013778.

Bunch T. E., Keil K., and Snetsinger K. G. 1967. Chromite composition in relation to chemistry and texture of ordinary chondrites. *Geochimica et Cosmochimica Acta* 31:1569–1582.

Eberhardt P., Geiss J., and Lutz H. 1963. Neutrons in meteorites. In *Earth science and meteoritics*, edited by Geiss J. and Goldberg E. D. Amsterdam: North Holland Publishing Company. pp. 143–168.

Edwards W. N. and Hildebrand A. R. 2004. SUPRACENTER: Locating fireball terminal bursts in the atmosphere using seismic arrivals. *Meteoritics & Planetary Science* 39:1449–1460.

Edwards W. N., Brown P. G., and ReVelle D. O. Forthcoming. Bolide energy estimates from infrasonic measurements. *Earth, Moon and Planets.*

Eugster O. 1988. Cosmic-ray production rates for He-3, Ne-21, Ar-38, Kr-83, and Xe-126 in chondrites based on Kr-81/Kr exposure ages. *Geochimica et Cosmochimica Acta* 52:1649–1662.

Eugster O., Michel Th., Niedermann S., Wang D., and Yi W. 1993. The record of cosmogenic, radiogenic, fissiogenic, and trapped

noble gases in recently recovered Chinese and other chondrites. *Geochimica et Cosmochimica Acta* 57:1115–1142.

Evans J. C., Reeves J. H., Rancitelli L. A., and Bogard D. D. 1982. Cosmogenic nuclides in recently fallen meteorites: Evidence for galactic cosmic ray variations during the period 1967–1978. *Journal of Geophysical Research* 87:5577–5591.

Evers L. G. and Haak H. W. 2001. Listening to sounds from an exploding meteor and oceanic waves. *Geophysical Research Letters* 28:41–44.

Evers L. G. and Haak H. W. 2003. Tracing a meteoric trajectory with infrasound. *Geophysical Research Letters* 30, doi:10.1029/2003GL017947.

Gomes C. B. and Keil K. 1980. *Brazilian stone meteorites.* Albuquerque: University of New Mexico Press. 161 pp.

Hedin A. E., Fleming E. L., Manson A. H., Schmidlin F. J., Avery S. K., Clark R. R., Franke S. J., Fraser G. J., Tsuda T., Vial F., and Vincent R. A. 1996. Empirical wind model for the upper, middle and lower atmosphere. *Journal of Atmospheric and Terrestrial Physics* 58:1421–1447.

Jarosewich E., 1990. Chemical analyses of meteorites–A compilation of stony and iron meteorite analyses. *Meteoritics* 25: 323–337.

Laubenstein M., Hult M., Gasparro J., Arnold D., Neumaier S., Heusser G., Köhler M., Povinec P., Reyss J.-L., Schwaiger M., and Theodórsson P. 2004. Underground measurements of radioactivity. *Applied Radiation and Isotopes* 61:167–172.

Le Pichon A., Guérin J. M., and Blanc E. 2002. Trail in the atmosphere of the 29 December 2000 meteor as recorded in Tahiti: Characteristics and trajectory reconstitution. *Journal of Geophysical Research* 107, doi:10.1029/2001JD001283.

Leya I., Lange H.-J., Neumann S., Wieler R., and Michel R. 2000. The production of cosmogenic nuclides in stony meteoroids by galactic cosmic ray particles. *Meteoritics & Planetary Science* 35:259–286.

Marti K. and Graf T. 1992. Cosmic-ray exposure history of ordinary chondrites. *Annual Review of Earth and Planetary Science* 20: 221–243.

Michel R. and Neumann S. 1998. Interpretation of cosmogenic nuclides in meteorites on the basis of accelerator experiments and physical model calculations. *Earth and Planetary Science* 107: 441–457.

Moffat A. F. J. 1969. A theoretical investigation of focal stellar images in the photographic emulsion and application to photographic photometry. *Astronomy and Astrophysics* 3:455–461.

ReVelle D. O. 1976. On meteor-generated infrasound. *Journal of Geophysical Research* 81:1217–1240.

ReVelle D. O. 1997. Historical detection of atmospheric impacts of large super-bolides using acoustic gravity waves. *Annals of the New York Academy of Sciences* 822:284–302.

Rubin A. E. 1985. Impact melt products of chondritic material. *Reviews of Geophysics* 23:277–300.

Rubin A. E. 1990. Kamacite and olivine in ordinary chondrites: Intergroup and intragroup relationships. *Geochimica et Cosmochimica Acta* 54:1217–1232.

Russell S. S., Folco L., Grady M. M., Zolensky M. E., Jones R., Righter K., Zipfel J., and Grossman J. N. 2004. The Meteoritical Bulletin, No. 88. *Meteoritics & Planetary Science* 39:A215–272.

Sisterson J. M., Kim K. J., and Reedy R. C. 2004. Revised production rates for ^{22}Na and ^{54}Mn in meteorites using cross sections measured for neutron-induced reactions (abstract #1354). 35th Lunar and Planetary Science Conference. CD-ROM.

Stöffler D., Keil D., and Scott E. R. D. 1991. Shock metamorphism of ordinary chondrites. *Geochimica et Cosmochimica Acta* 55: 3845–3867.

Tang M. and Anders E. 1988. Isotopic anomalies of Ne, Xe, and C in meteorites. III. Local and exotic noble gas components and their interrelations. *Geochimica et Cosmochimica Acta* 52:1245–1254.

Trigo-Rodríguez J. M., Borovicka J., Spurny P., Ortiz J. L., Docobo J. A., Castro-Tirado A. J., and Llorca J. Forthcoming. The Villalbeto de la Peña meteorite fall: II. Determination of the atmospheric trajectory and orbit. *Meteoritics & Planetary Science*.

van Schmus W. R. and Ribbe P. H. 1968. The composition and structural state of feldspar from chondritic meteorites. *Geochimica et Cosmochimica Acta* 32:1327–1342.

Welten K. C., Caffee M. W., Leya I., Masarik J., Nishiizumi K., and Wieler R. 2003. Noble gases and cosmogenic radionuclides in the Gold Basin L4-chondrite shower: Thermal history, exposure history, and pre-atmospheric size. *Meteoritics & Planetary Science* 38:157–174.

Wilkinson S. L. and Robinson M. S. 2000. Bulk density of ordinary chondrite meteorites and implications for asteroidal internal structure. *Meteoritics & Planetary Science* 35:1203–1213.